

Phase Transitions of Interacting Elastic Defects

Clare C. Yu

Physics Department, University of California, Irvine, California 92717

(Received 12 June 1992)

We have investigated a model of randomly placed defects with internal degrees of freedom which interact via elastic strain fields. Monte Carlo simulations and finite-size scaling indicate that two spin-glass phase transitions occur: one for the diagonal components of the defect stress tensor and the other for the off-diagonal components. The quenched ground state of the off-diagonal components exhibits antiferroelastic correlations while the diagonal components do not. We predict the fourth-order elastic susceptibilities associated with the defects diverge at the transition temperatures.

PACS numbers: 61.42.+h, 61.70.Yq, 75.50.Lk, 75.40.Mg

Defects in solids have long been studied as a model of how disorder affects physical properties. In this paper we study the question of whether a system of interacting defects with internal degrees of freedom has a phase transition [1]. In particular we consider randomly placed defects interacting with each other via the dipolar elastic strain field in three dimensions. From Monte Carlo simulations and finite-size scaling, we find that such a system undergoes two phase transitions in which degrees of freedom freeze out as the system is cooled. Representing the defects by stress tensors, we find that the diagonal components of the stress tensor undergo a spin-glass phase transition at a slightly higher temperature than the off-diagonal components. "Diagonal" and "off-diagonal" refer to the projection $\sigma_{\alpha\beta}\hat{x}_\alpha\hat{x}_\beta$ of the stress tensor on the (cubic) axes of the underlying lattice. In the quenched ground state, the off-diagonal components have planar antiferroelastic correlations while the diagonal components have none. We predict these two transitions would be associated with diverging fourth-order elastic susceptibilities. To our knowledge, this is the first time fourth-order elastic susceptibilities have been predicted to diverge.

We start by considering defects that couple linearly to the strain field:

$$H = \sigma_{\alpha\beta}(\mathbf{r})\varepsilon_{\alpha\beta}(\mathbf{r}), \quad (1)$$

where $\varepsilon_{\alpha\beta}(\mathbf{r})$ is the symmetric strain field and $\sigma_{\alpha\beta}(\mathbf{r})$ is the stress field associated with the defects. The indices α and β range over the real space directions x , y , and z , and the sum over repeated indices is understood. As in the two-level system (TLS) model of glasses [2], we assume that the defects have internal degrees of freedom. Thus $\sigma_{\alpha\beta}$ can be replaced by $\Gamma_{\alpha\beta}\cdot\mathbf{S}$ where \mathbf{S} is a spinlike TLS operator represented by Pauli matrices. $\Gamma_{\alpha\beta}$ is a vector in spin space and a matrix in real space. The spin representation is that of the energy eigenstates of the two-level system. S_x and S_y are operators for transitions between energy levels, while S_z does not involve transitions and is Ising-like.

The defects interact with each other via the elastic strain field. For simplicity we just consider the effective

$S_z S_z$ interaction which does not involve frequency-dependent effects.

Using either elasticity theory [3] or second-order [4,5] perturbation theory to eliminate the strain field yields

$$H_{\text{eff}}(\mathbf{r} - \mathbf{r}') = - \sum_{\lambda, \mathbf{k}} \frac{1}{\rho v_\lambda^2} \cos[\mathbf{k} \cdot (\mathbf{r} - \mathbf{r}')] \times \eta_{\alpha\beta}^{(\lambda)} \eta_{\gamma\delta}^{(\lambda)} \sigma_{\alpha\beta}(\mathbf{r}) \sigma_{\gamma\delta}(\mathbf{r}'), \quad (2)$$

where $\eta_{\alpha\beta}^{(\lambda)} = (\hat{k}_\alpha \hat{e}_\beta^{(\lambda)} + \hat{k}_\beta \hat{e}_\alpha^{(\lambda)})/2$. The sum over λ is over the longitudinal and transverse phonon polarizations. ρ is the density and v is the speed of sound. \hat{k}_α is the α th component of the unit phonon wave vector and \hat{e}_β is the β th component of the unit phonon polarization vector. Summing over k results in a dipolar interaction that roughly goes as g/r^3 where $g \sim \gamma^2/\rho v^2$ and γ is the order of magnitude of the defect stress. Taking $\gamma \sim 1$ eV, we estimate $g \sim 5 \times 10^4$ K \AA^3 for amorphous SiO_2 [6,7].

We simulate the system by placing defects randomly on the sites of a simple cubic lattice. A typical defect concentration is 25% and lattice sizes were 4^3 , 6^3 , and 8^3 . The energy scale is given by $J \sim g/a^3$ where a is the average defect-defect distance. This interaction energy is invariant under block scaling; since the stress of a block scales as \sqrt{N} , where N is the number of defects in the block, g scales as N , and J is invariant. We mimic the defect degrees of freedom by setting the magnitude of the stress couplings to 1 eV, say, but allowing the sign of each spatial stress component $\sigma_{\alpha\beta}$ to vary. In terms of $\Gamma_{\alpha\beta}\cdot\mathbf{S}$ this is tantamount to replacing \mathbf{S} by the magnitude of its matrix element and treating each component of $\Gamma_{\alpha\beta}$ like a fixed-length Ising spin. Since $\sigma_{\alpha\beta}$ is symmetric, there are six such components. Allowing the stress couplings to vary models the ability of a defect to respond to fluctuations in its local strain field due to temperature and the fluctuations of its neighbors. In the numerical simulations the defect stresses are flipped according to the standard heat bath Monte Carlo algorithm using the Hamiltonian (2) [8].

The local field of a defect is determined by summing over near-neighbor defects out to a distance of $R_c = \sqrt{5}a_0$ where a_0 is the lattice spacing. We believe that neglecting further neighbors does not change our results qualita-

tively for several reasons. First the angular integrals vanish as the stress due to far away defects becomes more isotropic. Second if the neglected defects were completely random and one neglects the angular integrals, the contribution to the local fields from the remaining defects goes roughly as $2g\sqrt{c}(R_c a_0)^{-3/2}$ where c is the fraction of sites occupied by defects. Since this is of order J for $c=25\%$, our calculations of the energy and the specific heat may be off by a factor of 2 or 3. Finally simulations on ordered systems ($c=1$) indicates that summing over 32 neighbors out to $2a_0$ vs 56 neighbors out to $\sqrt{5}a_0$ results in almost no change in the ground-state energy per defect and the temperature at which the specific-heat peak occurs. The ground-state configurations in both cases are antiferroelastic with the off-diagonal stress components exhibiting planar antiferroelasticity. An example is shown in Fig. 1. The ground state is not unique, since the symmetry of the Hamiltonian allows up to 24 degenerate configurations, though some of these can be identical.

Interestingly, the tendency for planar antiferroelasticity survives in the quenched ground state of the disordered case. The metastable ground state is obtained by taking the lowest-energy configuration found at a given temperature and aligning defect stresses along their local fields. The Fourier transform of the stress components quenched from the lowest temperatures is then taken and averaged over 50–100 samples. For a 25% concentration of defects the magnitude of the Fourier transform of the off-diagonal stress components $|\sigma_{\alpha\beta}(k)|$ has a peak at $ka_0=\pi$ in the quenched ground state while the diagonal components do not show any signs of ordering. The same features are present for 10% concentration but the peak height is reduced by a factor of 3 or 4, indicating reduced correlations with increasing dilution. Since the peak only involves one wave vector in both cases, this implies that the antiferroelastic correlation length is at least as large as the system size L .

In order to study the phase transition, we define a di-

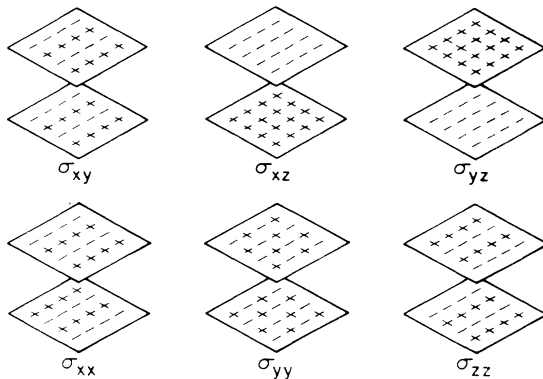


FIG. 1. An example of a ground-state stress configuration in the ordered case. Note the antiferroelastic correlations.

mensionless order parameter $g_{\alpha\beta}$ analogous to that used in spin glasses by Bhatt and Young [9],

$$g_{\alpha\beta} = \frac{1}{2} \left[3 - \frac{\langle q_{\alpha\beta}^4 \rangle}{\langle q_{\alpha\beta}^2 \rangle^2} \right], \quad (3)$$

where the n th moment of the stress overlap $q_{\alpha\beta}$ is given by

$$\langle q_{\alpha\beta}^n \rangle = \frac{1}{N^n(\tau_0+1)} \left[\sum_{t=0}^{\tau_0} \left(\sum_i \sigma_{\alpha\beta}(\mathbf{r}_i, t_0) \sigma_{\alpha\beta}(\mathbf{r}_i, t_0+t) \right)^n \right]_{\text{avg}}. \quad (4)$$

Since the dipolar interaction is not random but rather is dictated by the relative positions of the defects, the average $[\dots]_{\text{avg}}$ is over different samples which have different placements of the defects. 50–100 samples are used to obtain an accuracy of a few percent in $g_{\alpha\beta}$. t_0 is an initial equilibration time and we choose $\tau_0=t_0$. Following Bhatt and Young [9], we monitored the approach to equilibration by comparing the sample-averaged overlap of a set of defects at different times with the sample-averaged overlap of two replicas of defects at the same time. These two overlaps overestimate and underestimate the correlations, respectively. Above the transition temperature these two values converge to the same value as the number of Monte Carlo steps is increased, signaling that equilibrium has been reached. Below the transition temperature convergence is hampered because the symmetry of the Hamiltonian allows degenerate metastable ground states with little or no overlap. In this case we accepted the single replica value of $g_{\alpha\beta}$ defined in (3) and (4) when the fluctuations that occurred in the value of $g_{\alpha\beta}$ were comparable to the standard deviation of the sample average. As a further check of equilibration, we calculated the specific heat from energy fluctuations and checked that values for larger systems agreed with those for smaller systems which were known to have equilibrated by the convergence procedure. 6000 Monte Carlo steps per defect were used to achieve equilibration for the smallest samples at the highest temperature while 200000 Monte Carlo steps were used for the largest samples at the lowest temperature.

As the size of the system $L^d \rightarrow \infty$, the order parameter $g_{\alpha\beta}$ varies between 0 and 1 as the temperature drops through T_c . According to the finite-size scaling ansatz, L/ξ is the only relevant parameter, where ξ is the correlation length. This implies $g_{\alpha\beta} = \bar{g}_{\alpha\beta}(L^{1/\nu}(T - T_c))$ where $\bar{g}_{\alpha\beta}$ is a scaling function and ν is the correlation length exponent. Figure 2 shows a plot of g_{xy} and g_{xx} for $L=4, 6$, and 8. The curves cross at T_c since $g_{\alpha\beta}(T_c)$ is independent of L . Notice that T_c is different for g_{xy} and g_{xx} since the curves cross at different temperatures. Fitting the data by the scaling function leads to $T_{c-}/J=0.32 \pm 0.02$ and $1/\nu=1.0 \pm 0.4$ for the off-diagonal components, and $T_{c+}/J=0.42 \pm 0.02$ and $1/\nu=0.9 \pm 0.4$ for the diagonal components (Fig. 2). T_c is lower for the off-diagonal components because their interactions are

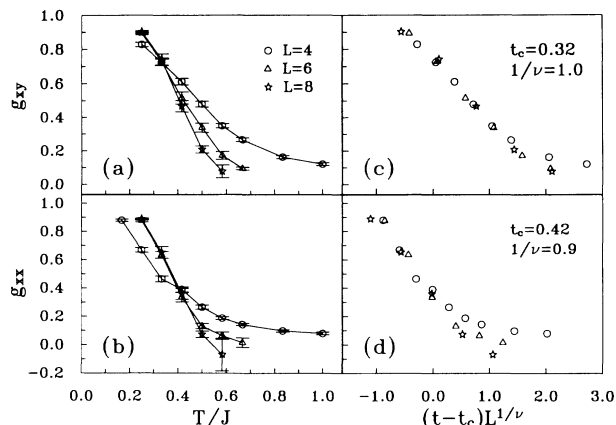


FIG. 2. (a) The xy component of the order parameter g_{xy} vs the reduced temperature $t = T/J$ for lattice sizes $L = 4, 6,$ and 8 . The concentration $c = 0.25$. The curves cross at $t_{c-} = T_{c-}/J$. The error bars at and above T_{c-}/J are the larger of half the difference between the final values of one- and two-replica correlations and the standard deviation from sample averaging. The error bars below T_{c-}/J are the standard deviation from single-replica sample averaging. (b) g_{xx} vs t . The curves cross at $t_{c+} = T_{c+}/J$. Notice that $t_{c+} > t_{c-}$. (c) g_{xy} fitted by the finite-size scaling formula with $t_{c-} = 0.32$ and $1/\nu = 1.0$. (d) g_{xx} scaled with $t_{c+} = 0.42$ and $1/\nu = 0.9$.

more frustrated than those of the diagonal components due to angular factors in terms such as $\hat{r}_i \hat{r}_j \hat{r}_k \hat{r}_l \sigma_{ij}(\mathbf{r}) \times \sigma_{kl}(\mathbf{r}')$, where \hat{r}_i is the i th component of the unit vector connecting the two defects. To see how the transitions depend on input parameters, we doubled the longitudinal velocity and found that the splitting between the transitions and $1/\nu$ did not change within the accuracy achieved.

Each transition is signaled by a divergence of the corresponding fourth-order elastic susceptibility $\chi_{\alpha\beta\alpha\beta\alpha\beta}$ associated with the defects. The susceptibilities are defined as the coefficients in an expansion of the thermodynamic stress per defect in powers of a small uniform external strain field $\varepsilon_{\alpha\beta}$. This divergence is completely analogous to the divergence of the spin-glass susceptibility at the spin-glass transition [10]. Our simulations indicate that the "spin-glass" susceptibility $\chi_{\alpha\beta}^{\text{SG}} = N \langle q_{\alpha\beta}^2 \rangle$ does indeed diverge. $\chi_{\alpha\beta}^{\text{SG}}$ is related to fourth-order elastic susceptibilities by $\chi_{\alpha\beta\alpha\beta\alpha\beta} = \beta^3 (\chi_{\alpha\beta}^{\text{SG}} - \frac{2}{3})$ where $\beta = 1/k_B T$. We have also found the exponent η , which describes the power-law decay of the correlation at T_c , by fitting with the finite-size scaling form $\chi_{\alpha\beta}^{\text{SG}} = L^{2-\eta} \chi_{\alpha\beta}^{\text{SG}}(L^{1/\nu}(T - T_c))$. This gives $\eta_- = -0.2 \pm 0.2$ for the off-diagonal components and $\eta_+ = +0.4 \pm 0.2$ for the diagonal components at $c = 25\%$. When the longitudinal velocity was doubled, η_- was closer to 0.2 but η_+ was still 0.4. The divergence of $\chi_{\alpha\beta}^{\text{SG}}$ goes as $[(T - T_c)/T_c]^{-\gamma}$ where $\gamma = (2 - \eta)\nu$.

Interacting defects have also attracted attention as a model for the low-temperature properties of glasses. In

particular the temperature range between 3 and 10 K is a crossover region characterized by a plateau in the thermal conductivity and a dramatic drop by a factor of 10^2 – 10^3 in C/T with decreasing temperature T . If we assume that phonons carry the heat in this temperature range [11], then the plateau represents a crossover from a short mean free path ($l \sim \lambda$) at high frequencies ($\nu > 200$ GHz) to a long mean free path ($l \sim 150\lambda$) at lower frequencies [12]. Attempts to explain this behavior have revolved around a drop with decreasing energy in the density of states which strongly scatter phonons [13]. This leads to a drop in the specific heat and a longer phonon mean free path at low energies. Indeed neutron [14] and Raman [15,16] scattering have seen evidence for this hole at temperatures well above the crossover temperature, though they have tended to probe frequencies and temperatures that are somewhat higher than those involved in the crossover. A model of interacting defects could explain this since interactions tend to increase unperturbed energy splittings and produce a hole in the density of states. However, a decrease in the density of states cannot easily explain why the ultrasonic attenuation at a fixed frequency decreases by roughly a factor of 30 as the temperature drops from 100 to 1 K. At low frequencies ($\nu \lesssim 1$ GHz) this has been attributed to relaxation and structural rearrangement [2]. At high frequencies [17] ($\nu \gtrsim 100$ GHz), however, structural relaxation is too slow to contribute and another explanation is needed. In particular there is the intriguing possibility that the crossover signals a phase transition in which degrees of freedom freeze out as the system is cooled [18].

We can test this hypothesis with our model. Note that for a mean defect-defect distance of $a \sim 15$ Å and $\gamma \sim 1$ eV, $T_c \sim J/3 \sim 5$ K which is the right order of magnitude for the crossover temperature. We have also calculated the contribution to the specific heat from the energy fluctuations of the defects. As a function of temperature, it is a broad bump that has a linear slope at low temperatures and a maximum at $T \approx J/2$. As in spin glasses [10], $T_{c\pm}$ occurs at a lower temperature than the maximum. The specific heat only increases by a factor of 2 from $T = 0.25$ J to 0.5 J which is much less than that seen experimentally between 3 and 10 K. Thus freezing due to instantaneous $1/r^3$ interactions is too mild to account for the low-temperature crossover seen in glasses. This implies that the Hamiltonian should include frequency-dependent interactions which involve defects making transitions between energy levels. There are some indications that such terms would lead to a greater drop in entropy upon freezing [7].

Finally we note that low-temperature thermal expansion and ultrasonic measurements on glasses indicate that defect stresses have a broad distribution centered very close to zero [19]. In particular the ratio of the average dilation stress per defect to the rms value of the stress $\langle Tr(\sigma)/3 \rangle / \langle \sigma^2 \rangle^{1/2} \sim 10^{-3}$, where $\langle \sigma^2 \rangle$ is averaged over all stress components. This is naturally explained in our

model by the presence of disorder. Averaging over 110 quenched ground states ($L=8$) we find that this ratio equals -0.003 ± 0.03 which is consistent with experiment.

To summarize, we have studied a system of elastically interacting defects. We find that the diagonal and off-diagonal components of the defect stress tensor undergo separate phase transitions. In the quenched ground state the off-diagonal components have antiferroelastic correlations. While some of these features may be a result of allowing the components of the stress tensor to represent independent degrees of freedom, the divergence of the fourth-order elastic susceptibilities should be valid for any elastic spin-glass transition such as occurs in $\text{KBr}_{1-x}\text{KCN}_x$.

I would like to thank Eric Grannan and Sue Coppersmith for helpful discussions. This work was supported in part by ONR Grant No. N000014-91-J-1502, the Petroleum Research Fund administered by the American Chemical Society, the Alfred P. Sloan Foundation, and an allocation of computer time from the University of California, Irvine.

-
- [1] A. Loidl, *Annu. Rev. Phys. Chem.* **40**, 29 (1989), and references therein.
 [2] Good reviews are *Amorphous Solids*, edited by W. A. Phillips (Springer, Berlin, 1981); and S. Hunklinger and A. K. Raychaudhuri, *Prog. Low Temp. Phys.* **9**, 265 (1986).
 [3] E. R. Grannan, M. Randeria, and J. P. Sethna, *Phys. Rev. Lett.* **60**, 1402 (1988); *Phys. Rev. B* **41**, 7784 (1990); **41**, 7799 (1990).

- [4] J. Joffrin and A. Levelut, *J. Phys. (Paris)* **36**, 811 (1975).
 [5] A. J. Leggett and C. C. Yu (unpublished).
 [6] C. C. Yu and A. J. Leggett, *Comments Condens. Matter Phys.* **14**, 231 (1988).
 [7] C. C. Yu, *Phys. Rev. Lett.* **63**, 1160 (1989).
 [8] We used amorphous SiO_2 values: $\rho=2.2 \text{ g/cm}^3$, $v_l=5.8 \times 10^5 \text{ cm/sec}$, and $v_t=3.75 \times 10^5 \text{ cm/sec}$.
 [9] R. N. Bhatt and A. P. Young, *Phys. Rev. B* **37**, 5606 (1988).
 [10] Good reviews are K. H. Fischer and J. A. Hertz, *Spin Glasses* (Cambridge Univ. Press, Cambridge, 1991); and K. Binder and A. P. Young, *Rev. Mod. Phys.* **58**, 801 (1986).
 [11] M. P. Zaitlin and A. C. Anderson, *Phys. Rev. B* **12**, 4475 (1975).
 [12] J. J. Freeman and A. C. Anderson, *Phys. Rev. B* **34**, 5684 (1986).
 [13] C. C. Yu and J. J. Freeman, *Phys. Rev. B* **36**, 7620 (1987); E. Akkermans and R. Maynard, *Phys. Rev. B* **32**, 7850 (1985); S. Alexander, O. Entin-Wohlman, and R. Orbach, *Phys. Rev. B* **34**, 2726 (1986); J. E. Graebner, B. Golding, and L. C. Allen, *Phys. Rev. B* **34**, 5696 (1986); J. E. Graebner and B. Golding, *Phys. Rev. B* **34**, 5788 (1986); V. G. Karpov and D. A. Parshin, *Zh. Eksp. Teor. Fiz.* **88**, 2212 (1985) [*Sov. Phys. JETP* **61**, 1308 (1985)]; P. Sheng and M. Zhou, *Science* **253**, 539 (1991).
 [14] U. Buchenau, M. Payer, N. Nücker, A. J. Dianoux, N. Ahmad, and W. A. Phillips, *Phys. Rev. B* **34**, 5665 (1986).
 [15] R. H. Stolen, *Phys. Chem. Glasses* **11**, 83 (1970).
 [16] M. Hass, *J. Phys. Chem. Solids* **31**, 415 (1970).
 [17] T. C. Zhu, H. J. Maris, and J. Tauc, *Phys. Rev. B* **44**, 4281 (1991).
 [18] R. O. Pohl, *Am. J. Phys.* **55**, 240 (1987); S. N. Coppersmith, *Phys. Rev. Lett.* **67**, 2315 (1991).
 [19] A. C. Anderson, *J. Non-Cryst. Solids* **85**, 211 (1986); *Phys. Rev. B* **34**, 1317 (1986).